A Practical Method for Optimum Seismic Design of Friction Wall Dampers

Neda Nabid,[a)] M.EERI, Iman Hajirasouliha,[b)] and Mihail Petkovski[c)]

Friction control systems have been widely used as one of the efficient and cost effective solutions to control structural damage during strong earthquakes. However, the height-wise distribution of slip loads can significantly affect the seismic performance of the strengthened frames. In this study, a practical design methodology is developed for more efficient design of friction wall dampers by performing extensive nonlinear dynamic analyses on 3, 5, 10, 15, and 20-story RC frames subjected to seven spectrum-compatible design earthquakes and five different slip load distribution patterns. The results show that a uniform cumulative distribution can provide considerably higher energy dissipation capacity than the commonly used uniform slip load pattern. It is also proved that for a set of design earthquakes, there is an optimum range for slip loads that is a function of number of stories. Based on the results of this study, an empirical equation is proposed to calculate a more efficient slip load distribution of friction wall dampers for practical applications. The efficiency of the proposed method is demonstrated through several design examples.

INTRODUCTION

Much of the existing building structures in developing countries are designed primarily to sustain gravity loads with little or no seismic detailing. Many catastrophic failures in RC buildings during recent major earthquakes (e.g. Kashmir, 2005; China, 2008; Indonesia, 2009; Haiti, 2010; Turkey, 2011; Nepal, 2015) have highlighted the urgent need to improve the seismic performance of these substandard buildings. Passive energy dissipation devices have been proven as one of the most efficient and cost effective solutions in terms of controlling structural damage during strong earthquakes by dissipating the imparted seismic energy and reducing damage in structural elements (Symans et al., 2008; Soong and

[a)] PhD Candidate, Department of Civil Engineering, The University of Sheffield, Sheffield, UK.
E-mail: nnabid1@sheffield.ac.uk (Corresponding Author)
[b)] Associate Professor, Department of Civil and Structural Engineering, The University of Sheffield, Sheffield, UK. E-mail: i.hajirasouliha@sheffield.ac.uk
[c)] Assistant Professor, Department of Civil and Structural Engineering, The University of Sheffield, Sheffield, UK. E-mail: m.petkovski@sheffield.ac.uk

Costantinou, 2014). Among the different types of passive energy dissipation devices, friction-based dampers usually have the highest energy dissipation capacity for the same levels of force and deformation (Pall and Pall, 2004). Moreover, friction devices are in general velocity and temperature-independent, can be easily tuned to the characteristics of the structure, and provide sustained performance under large number of cycles (Grigorian et al., 1993, Aiken et al., 1993, Pall and Pall, 2004).

Pall and Marsh (1982) introduced the first generation of friction dampers for braced steel frames, which were designed to slip under a predetermined load before the buckling of the braces occurred. Wu et al. (2005) developed an improved model of Pall friction dampers using a T-shaped core plate, which was easier to manufacture and assembly. Slotted Bolted Connections (SBC) were initially used by Fitzgerald (1989) to dissipate earthquake input energy and prevent buckling of brace elements in steel braced frames. The energy absorbing mechanism in SBCs is based on the friction between the gusset plates and the sliding channels. More recently, shear slotted bolted connections (SSBC) were proposed to extend the application of SBC in members with shear-dominated behavior (Nikoukalam et al., 2015).

While most of existing friction-based dampers were developed for steel bracing systems, using brace elements in RC frames can lead to high stress concentration and damage in the connection zones. This problem can be addressed by using wall-type systems that provide enough space to transfer lateral forces to the adjacent elements. Sasani and Popov (1997) experimentally and analytically investigated the performance of a wall-type friction damper using lightweight concrete panels. Their proposed system consisted of a precast concrete wall which was connected to the lower floor beam by bolted supports and to the upper floor beam by friction energy dissipating connectors. In a follow up study, they increased the efficiency of their proposed system by using epoxy-anchored bolts to provide adequate strength and stiffness at the base supports to minimize the rocking movement of the wall panels during strong earthquakes (Sasani and Popov, 2001). Petkovski and Waldron (2003) studied the effectiveness of friction-based concrete wall dampers (with and without opening) to improve the seismic performance of 6, 8 and 10-story RC structures subjected to four real earthquake records. They concluded that, irrespective of the stiffness of the wall panels, there was an optimum range for the slip force in the friction connections that led to the best seismic performance. Although their proposed friction wall dampers were designed not to transfer additional shear forces to the adjacent columns, the results of their study showed that they still considerably increase the base shear and the axial loads of the columns. However, these adverse effects can be controlled by limiting the slip forces in the friction dampers as it will be discussed in this study. A similar wall friction damper was proposed by Cho and Kwon (2004), incorporated an RC wall connected to the upper floor beam using a T-shape steel device with Teflon sliding sheets. In their system, the clamping force could be easily adjusted based on the expected earthquake magnitude using an oil jack loading system.

While several research studies have covered the optimum design of viscous and viscoelastic dampers (e.g. Park et al. 2004, Levy and Lavan 2006, Takewaki 2011, Whittle et al. 2012, Adachi et al. 2013, Sonmez et al. 2013), very limited studies are focused on the optimization of friction-based dampers subjected to seismic actions. In one of the early attempts, Filiatrault and Cherry (1990) proposed a simplified seismic design procedure to obtain the optimum slip load values by minimizing an energy derivation parameter denoted as relative performance index (RPI). It was shown that the optimum slip load values depend more on the amplitude and frequency of the design earthquake rather than the structural characteristics. Subsequently, Moreschi and Singh (2003) used Genetic Algorithm (GA) to determine the optimum height-wise placement of yielding metallic and friction dampers in braced steel frames. Patro and Sinha (2010) investigated the seismic performance of shear-frame building structures with dry-friction devices, using uniform height-wise slip load distribution. They showed that, in general, a suitable slip load range can be determined such that the seismic response of the structure is nearly optimal for a wide range of ground motion characteristics. Fallah and Honarparast (2013) optimized the slip load distribution and placement of Pall friction dampers in multi-story shear braced frame using a non-dominated sorting genetic algorithm (NSGA-II). In a more recent study, Miguel et al. (2016) adopted a backtracking search optimization algorithm to simultaneously optimize the location and slip load distribution of friction dampers subjected to seismic loading.

It should be noted that most of the above mentioned optimization techniques may not be suitable for practical design purposes due to the high computational efforts required to analyze a large number of non-linear dynamic systems. This study aims to develop, for the first time, a practical method for more efficient design of friction-based wall dampers under earthquake loads without using complex optimization techniques. To obtain the best slip load distribution along the height of the building, extensive nonlinear dynamic analyses are conducted on 3, 5, 10, 15, and 20-story RC frames subjected to a set of earthquake records representing a design spectrum. The results are then used to develop an empirical design equation, which leads to design solutions with maximum energy dissipation in the friction wall dampers. The efficiency of the proposed equation is demonstrated through several design examples.

MODELING AND ASSUMPTIONS

REFERENCE FRAMES

In this study 3, 5, 10, 15 and 20-story RC frames were selected with the typical geometry shown in Figure 1. The frames were assumed to be located on a soil type D of the IBC (2015) category, with the design spectral response acceleration at short periods and 1-sec period equal to 0.40g and 0.64g, respectively. To represent substandard RC structures, the frames were designed based on the low-to-medium seismicity regions using a design earthquake with PGA of 0.2g. The uniformly distributed dead and live loads were assumed as 6 kN/m^2 and 2 kN/m^2 for interior stories, and 5 kN/m^2 and 1.5 kN/m^2 for the roof level. The frames were designed to support the seismic loads based on IBC (2015) and ASCE/SEI 7-10 (2010) and in accordance with the minimum requirements of ACI 318 (2014) for RC frames with intermediate ductility. The concrete compressive strength (f_c') and the yield strength of steel reinforcement bars (f_y) were assumed to be 35 and 400 Mpa, respectively. Square and rectangular sections were used for column and beam elements as shown in Figure 1 for the 10-story frame.

To predict the seismic response of the RC frames, nonlinear time-history analyses were carried out using computer program DRAIN-2DX (Prakash et al. 1993). Rayleigh damping model with a constant damping ratio of 0.05 was assigned to the first mode and to any mode at which the cumulative mass participation exceeded 95%. Nonlinear moment-rotation (M-θ) and axial-moment (P-M) plastic hinges were assigned at both ends of RC beam and column elements, respectively, using element Type 2 in DRAIN-2DX. The friction mechanism at the top edge of the panel was modeled by means of an inelastic link element (element Type 4 in DRAIN-2DX) to provide an ideal Coulomb friction hysteretic behavior. In this study, it was assumed that the strength of the concrete wall panel is always greater than the effects of the maximum slip load of the friction device. Therefore, the wall panels were modeled with elastic panel elements (15 cm thickness) using element Type 6 in DRAIN-2DX. To consider rigid diaphragms in the analytical models, the frames nodes were constrained to each other in horizontal direction.

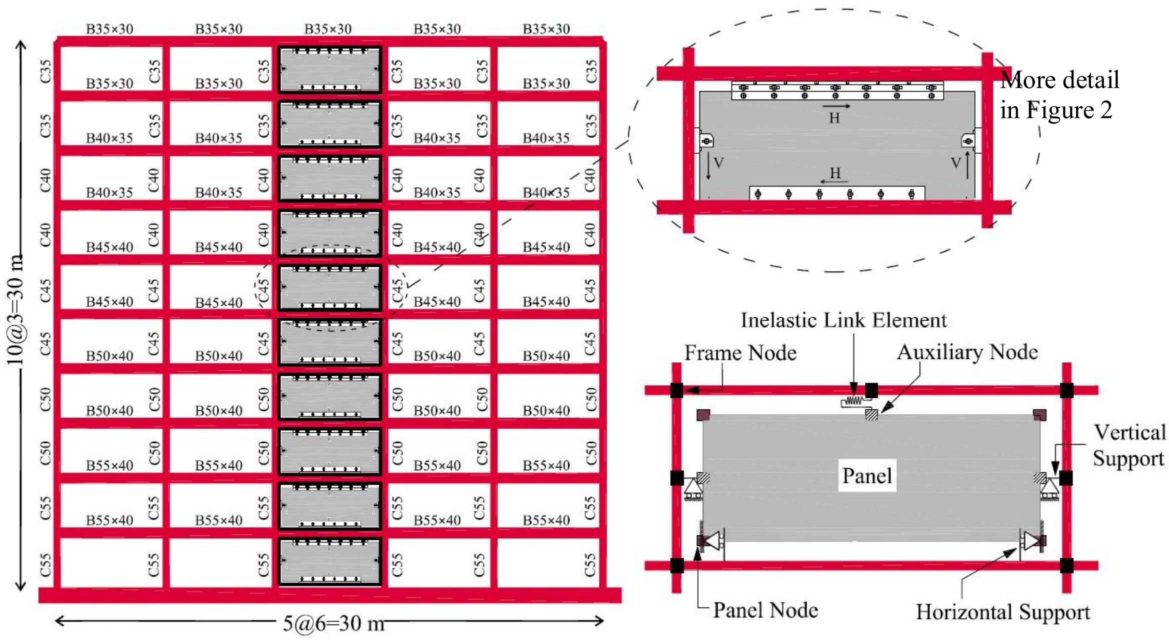

Figure 1. Schematic geometry of the reference RC frames and the analytical model of the studied friction-based wall dampers

PROPOSED FRICTION-BASED WALL DAMPER

The friction-based wall damper used in this study consists of a structural concrete panel that is connected to the frame by using two vertical supports in the sides, one horizontal connection at the bottom, and a friction device at the top. Figure 2 illustrates the details of the proposed friction panel. The vertical support for the concrete panel is provided by using panel-to-column connections with horizontal slots, which prevent transfer of shear forces to the columns. The panel is connected to the lower floor by horizontally fixed connections with vertical slots to avoid transferring shear forces to the beams. This arrangement will ensure that the displacement of the friction device at the top of the panel is equal to the inter-story drift at each level. The proposed friction device is a simple panel-to-frame Slotted Bolted Connection, which consists of two steel plates bolted at the top of the panel (external plates) clamped together over a slotted stainless steel plate anchored to the top beam (central plate). The friction mechanism is obtained through friction between the central stainless steel plate and the two brass plates (see Figure 2 (b)). Extensive experimental tests conducted by Grigorian et al. (1993) demonstrated the reliable hysteretic behavior of this type of friction device under sinusoidal and simulated seismic imposed displacements.

By using over-sized holes in the central steel plate (as shown in Figure 2), the largest friction forces will occur between the central and the brass plates. The size of these holes in the horizontal and vertical directions can be calculated to accommodate the expected maximum lateral drift and vertical deformations of the beam, which would prevent transfer of large stresses on the central plate around the slotted holes. The concentrated moments applied to the columns at the location of the connections should be considered in the design process of the proposed friction wall system. The results of this study indicate that these additional loads are relatively low compared to the maximum bending moments in the corresponding bare frame.

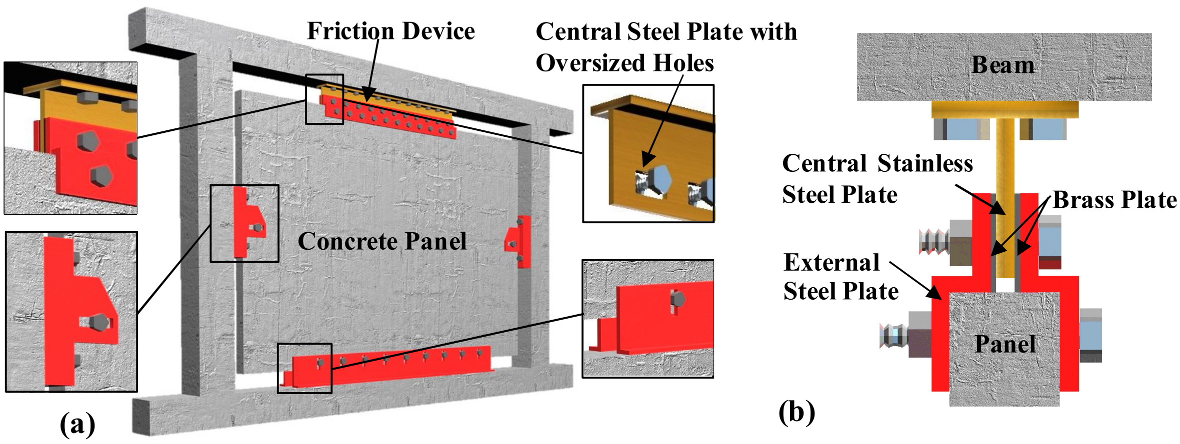

Figure 2. Schematic view of the (a) proposed friction wall damper, (b) friction device

SLIP LOAD DISTRIBUTION PATTERNS

The slip force in the friction connections of the proposed wall damper can be adjusted and tuned independently for each story by controlling the clamping forces of the bolts. Such capability provides the possibility of using the same connection with optimized slip loads. Wall dampers with very low slip loads (i.e. $F_s \cong 0$) do not have any lateral load resistance and, therefore, are not considered as structural elements. On the contrary, using large slip load values may lead to a connection lock-up under design earthquakes, which implies the passive control system behaves as a fixed wall panel with negligible energy dissipation capacity. In practical applications, a uniform height-wise slip load distribution is usually employed for design of passive friction dampers. However, this may not necessarily lead to an optimum design solution for a range of structures and design earthquakes.

To identify more efficient slip load distributions, five different distribution patterns are considered: (1) uniform, (2) uniform cumulative, (3) triangular cumulative, (4) inverted triangular cumulative and (5) a distribution proportional to the story shear strengths. Figure 3 shows the different slip load distribution patterns, scaled to produce the same base shear in first mode response (i.e. ΣF_s=constant). The shear strength of each story ($F_{y,i}$) can be calculated from a non-linear pushover analysis (Hajirasouliha and Doostan, 2010).

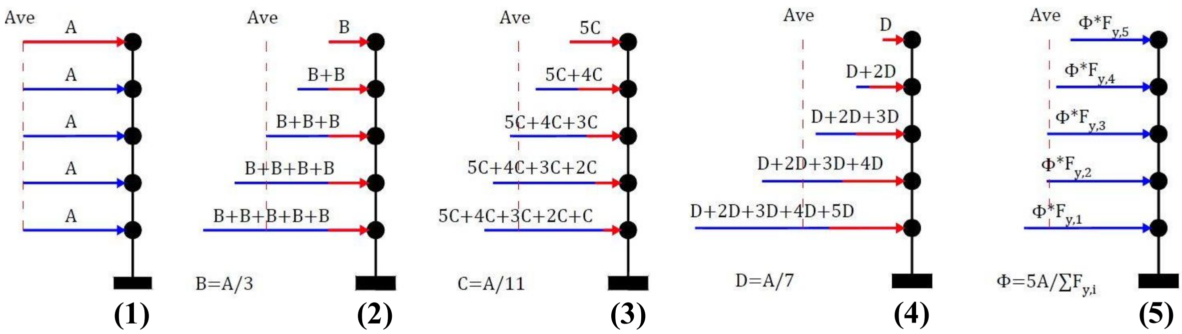

Figure 3. Typical patterns of the selected slip load distributions with the same average value

SELECTED SEISMIC EXCITATIONS

The reference structures are subjected to six real strong ground motions: Cape Mendocino 1992, Duzce 1999, Superstition Hills 1987, Imperial Valley 1979, Loma Prieta 1989, and Northridge 1994. The characteristics of the selected records are listed in Table 1. All of these ground motions correspond to soil class D of IBC-2015 and are recorded in low to moderate distances from the epicenter (less than 45 km) with high local magnitudes (i.e. M>6.5).

Table 1. Characteristics of the selected seismic excitation records

No.	*Earthquake Name*	*M*	*Record*	*Duration (s)*	*PGA (g)*	*PGV (Cm/s)*	*PGD (Cm)*
1	1992 Cape Mendocino	6.9	CAPEMEND/PET000	36	0.590	48.4	21.74
2	1999 Duzce, Turkey	7.2	DUZCE/DZC270	26	0.535	83.5	51.59
3	1987 Superstition Hills (B)	6.7	SUPERST/B-ICC000	60	0.358	46.4	17.50
4	1979 Imperial Valley	6.5	IMPVALL/H-E04140	39	0.485	37.4	20.23
5	1989 Loma Prieta	6.9	LOMAP/G03000	40	0.555	35.7	8.21
6	1994 Northridge	6.7	NORTHR/NWH360	40	0.590	97.2	38.05

Figure 4 illustrates the 5% damped elastic acceleration response spectra of the six natural earthquake records in Table 1. It is shown that, on average, the selected ground motions provide a close approximation to the design response spectra of IBC-2015 for the site class D in high seismic zones (i.e. PGA=0.4g). This is particularly evident at the first mode periods of the bare frames denoted as Tb3 to Tb20. Therefore, in this study these earthquake records are used directly without being normalized. A set of five synthetic earthquake records with a PGA of 0.4 g is also generated using SIMQKE program (Vanmarke, 1976) to be compatible with the soil type D of IBC (2015) elastic design spectrum. To simulate non-stationary spatially variable ground motions, a trapezoidal intensity envelope function with the rise time, level time and total duration of 2.5, 12 and 35 sec, respectively, was applied. Figure 4 demonstrates a good compatibility between the average spectrum of the synthetic earthquakes and the IBC (2015) design spectrum. Therefore, these synthetic earthquakes can be considered to be good representatives of the design response spectrum.

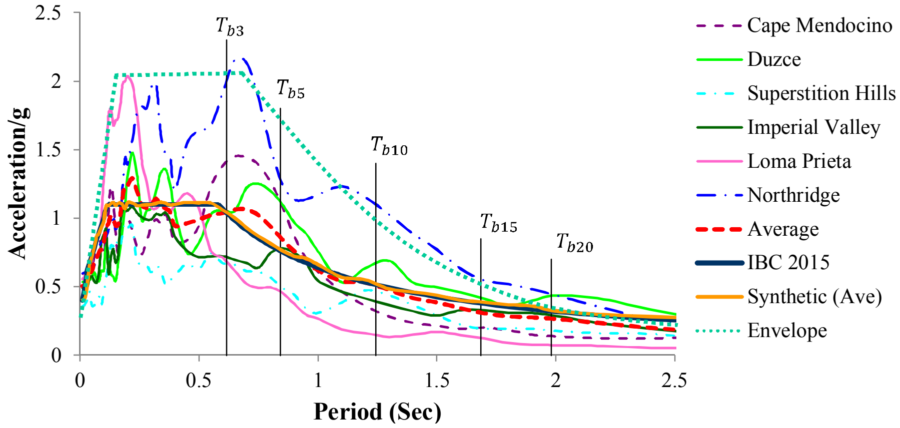

Figure 4. Comparison between elastic spectral acceleration of the six selected earthquakes, average of five synthetic earthquakes and IBC-2015 design spectrum for soil type D, 5% damping ratio. Tb3 to Tb20 are first mode periods of the bare frames

RC FRAMES WITH FRICTION-BASED WALL DAMPERS

To investigate the efficiency of the proposed passive-control system, a wide range of slip load values and height-wise distribution patterns are considered, aiming to cover all practical design solutions. Different structural performance parameters such as maximum inter-story drift, roof displacement, maximum axial load in columns, base shear, and cumulative energy dissipation are calculated. For comparison purposes, the slip load ratio F_{SR} is defined as:

$$F_{SR} = \frac{\sum_{i=1}^{n} F_{s,i}}{\sum_{i=1}^{n} F_{y,i}} \tag{1}$$

where n is number of stories, $F_{s,i}$ is slip force at i^{th} story, and $F_{y,i}$ is story shear strength of the i^{th} story. Using this parameter helps to compare the effects of using different slip load distributions, while the base shear force remains constant.

MAXIMUM INTER-STORY DRIFT

Maximum inter-story drift is widely used to evaluate the level of damage to both structural and non-structural elements in RC structures (Hajirasouliha et al. 2012). Figure 5 shows the variation of maximum inter-story drift ratios (normalized to the bare frames) for 5, 10, 15 and 20-story frames using five different slip load distribution patterns with a wide range of slip load ratios F_{SR}. The results are the average of the displacement demands obtained in the six selected earthquakes listed in Table 1. The energy dissipation capacity of wall panels with very small F_{SR} values is negligible, and therefore, their response is close to that of bare frames (normalized response parameters are close to 1.0). Figure 5 demonstrates a similar trend for different slip load patterns, where the maximum drift ratios generally reduce by increasing the friction slip load ratios up to a certain limit. This is followed by a constant trend in 3 and 5-story and an ascending trend in 10, 15 and 20-story frames.

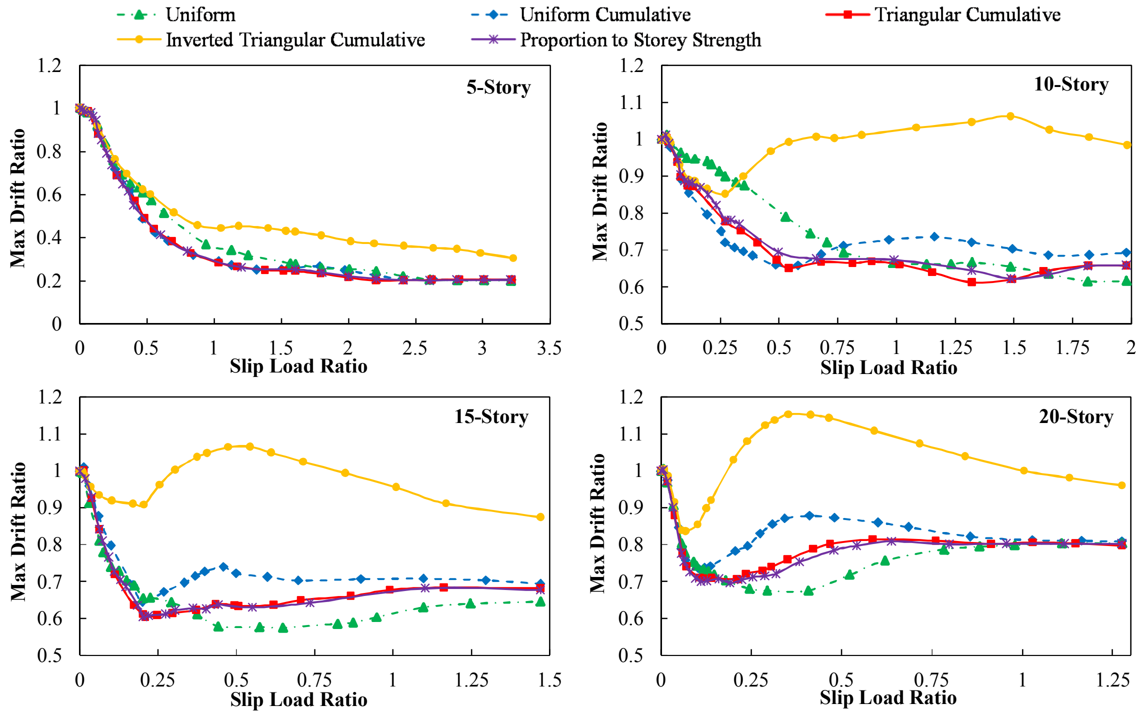

Figure 5. Variation of maximum inter-story drift for 5, 10, 15 and 20-story RC frames using different slip load distributions, average of the six selected earthquakes

The results in Figure 5 indicate that there is an optimum range for slip load ratios that, on average, leads to lower inter-story drifts. Similar conclusions have been reported by Petkovski and Waldron (2003) and Fallah and Honarparast (2013) for other types of friction dampers. Figure 5 shows that by using friction wall dampers with more efficient slip load distributions, the maximum inter-story drift of 3, 5, 10, 15, and 20-story frames reduced by up to 85%, 75%, 38%, 40%, and 30%, respectively. This implies that the reduction in maximum drift ratio is more prominent in low rise buildings. While the inverted triangular cumulative slip load distribution (Type 4 in Figure 3) seems to be less effective in reducing maximum inter-story drifts, other distribution patterns lead to similar levels of reduction.

COLUMN AXIAL LOAD

Figures 6 (a and b) display the maximum axial load ratios (normalized to the bare frames) of the columns connected to the friction wall dampers in 10 and 20-story frames using different slip load ratios. The results show that, regardless of the selected slip load distribution pattern, the maximum axial load in the columns increases by increasing the slip load ratios up to a steady-state level (see Figure 6 (b)). At this stage, the wall dampers are locked at all story levels, which is referred to as "fixed-wall" in this study. As expected, increasing slip load ratios beyond this limit does not affect the seismic performance of the frames. It is shown that, for the same slip load ratio, using uniform distribution (Type 1 in Figure 3) results in lower axial loads compared to other slip load distributions. However, for practical design purposes, it is important to obtain slip load ratios that control the lateral displacement demands of the structure without imposing high axial loads to the columns and foundations. Figures 7 (a and b) compare the maximum column axial load ratio for different slip load distributions as a function of maximum inter-story drift. The results in general indicate that, for a specific inter-story drift, using a uniform cumulative distribution (Type 2 in Figure 3) leads to minimum axial loads compared to other slip load distributions. A similar trend was observed for the other frames with different number of stories.

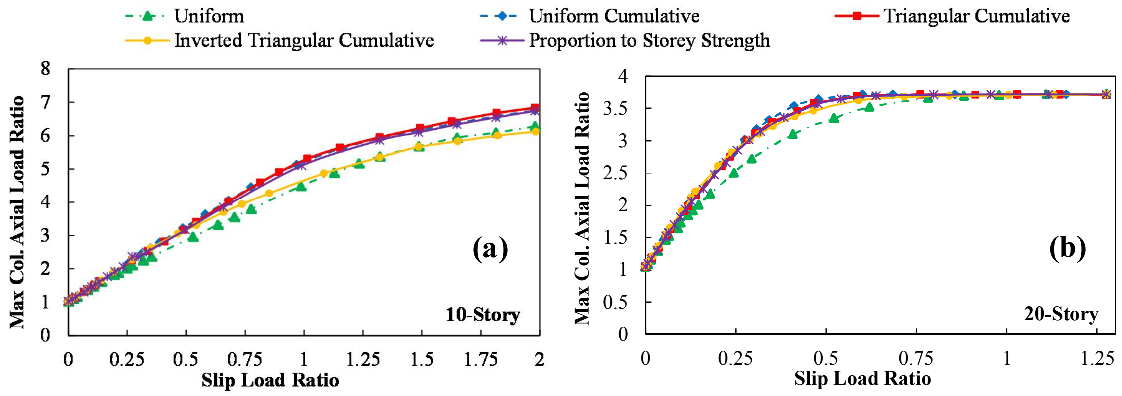

Figure 6. Variation of maximum column axial load ratio as a function of slip load ratio for (a) 10 and (b) 20-story frame, average of the six selected earthquakes

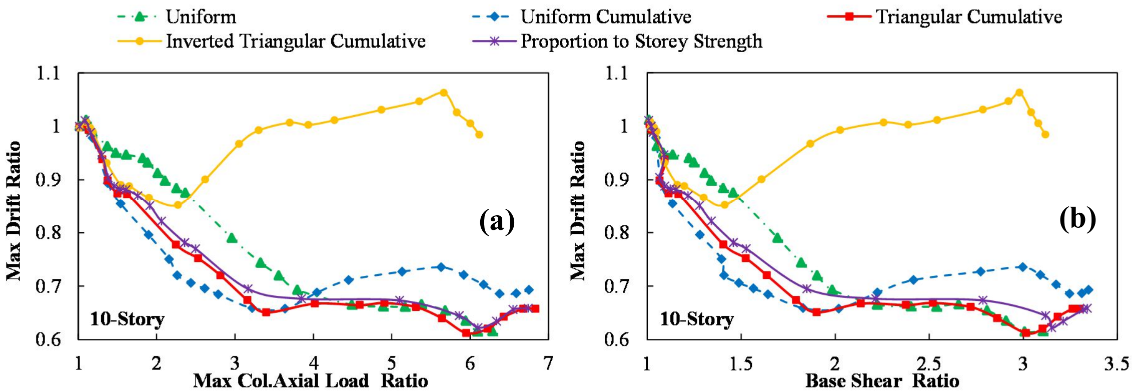

Figure 7. Variation of maximum drift ratio as a function of (a) column axial load and (b) base shear ratio for 10-story frame, average of the six selected earthquakes

BASE SHEAR

Increasing the base shear demand is one of the main barriers to the use of passive control systems such as shear walls and bracings. Although the proposed friction wall damper increases the base shear demand of the bare frame, this increase can be efficiently controlled by using appropriate slip loads in friction devices. For example, Figure 8 (a) compares the base shear and the maximum column shear force ratios of 10-story frames with different slip load distributions as a function of the slip load ratio. The results show that increasing the slip loads is always accompanied by an increase of the base shear until a maximum level is reached. For similar slip load ratios, using uniform slip load distribution leads to lower base shear when compared with other distribution patterns. However, for the same inter-story drift ratios, uniform cumulative slip load distribution in general leads to lower base shear values compared to the other distribution patterns (see Figure 7 (b)).

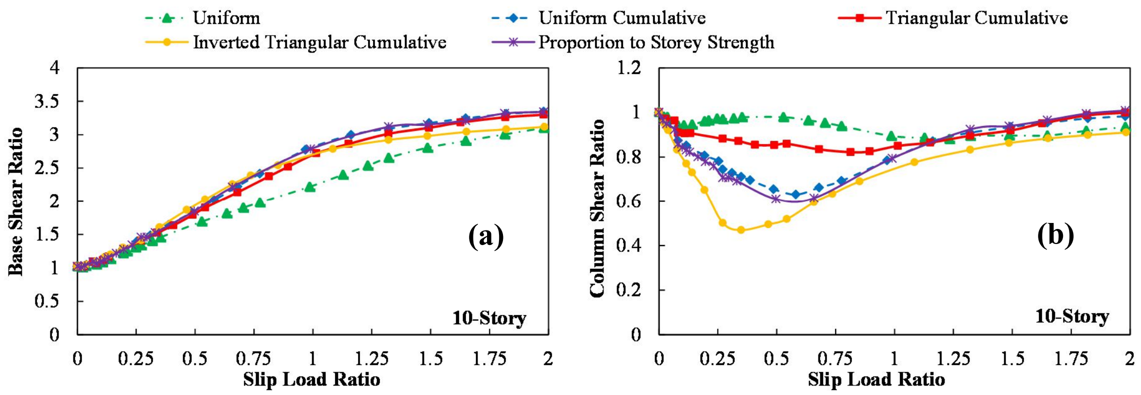

Figure 8. Variation of: (a) maximum column shear force ratio, and (b) base shear ratio as functions of slip load ratio, 10-story frame, average of the six selected earthquakes

It should be noted that the proposed friction wall damper is capable of transferring some of the base shear forces directly to the foundation at the ground floor. Therefore, despite increasing the total base shear, the proposed wall dampers can generally reduce the maximum shear forces in the columns at the base of the structure. For instance, the results in Figure 8 (b) indicate that unlike the base shear, increasing the slip load ratio is usually accompanied by a decrease in the maximum column shear forces until a minimum value is reached.

The most reduction in the maximum column shear forces was observed in the frame with the inverted triangular cumulative pattern (Type 4 in Figure 3). The main reason is that, for the same average slip load, the inverted triangular pattern has larger slip load values at the ground floor. This implies that the friction wall system can transfer higher shear forces directly to the foundation, which reduces the maximum shear forces at the columns.

ENERGY DISSIPATION CAPACITY

In this study, R_{w1} is defined as the ratio of the deformation work of structural elements in the structure with friction wall dampers (W_{cs}) to that in the corresponding bare frame (W_{bf}):

$$R_{w1} = \frac{W_{cs}}{W_{bf}} = \frac{(W_{sb} + W_{sc})_{cs}}{(W_{sb} + W_{sc})_{bf}} \tag{2}$$

where W_{sb} and W_{sc} denote the static work of the beam and column elements, respectively. R_{w1} decreases by increasing the efficiency of the friction wall dampers in dissipating the earthquake input energy. Figure 9 (a) shows the R_{w1} as a function of the slip load ratio for 3, 5, 10, 15 and 20-story frames using different slip load distribution patterns. In general, R_{w1} reaches a minimum value at a slip load ratio which is almost independent of the selected slip load distribution pattern. This implies that there is an optimum range for the slip load ratios that leads to the lowest deformation work (or structural damage) in the structural elements. The reduction in R_{w1} is more evident in low- to medium-rise buildings. The results also indicate that the optimum slip force ratios decrease by increasing the number of stories (from F_{SR}=1 in 3-story to F_{SR}=0.15 in 20-story frames). Also it can be noted that, in general, the optimum range narrows by increasing the number of stories.

The amount of energy dissipated in the friction device under a design earthquake can be evaluated by calculating the ratio of the friction work in the wall dampers (W_{sf}) to the deformation work of the main structural elements (W_{cs}):

$$R_{w2} = \frac{(W_{sf})_{cs}}{(W_{sb} + W_{sc})_{cs}} \tag{3}$$

While R_{w1} gives a measure of the efficiency of the dampers in reducing the energy dissipation demand of the structural elements, R_{w2} represents the energy dissipation capacity of the dampers. The variation of R_{w2} as a function of the slip load ratio is illustrated in Figure 9 (b) for 3, 5, 10, 15 and 20-story frames. The R_{w2} parameter tends to zero for very low and very high slip forces. The reason is that the energy dissipated in the dampers with very low slip forces is negligible, while the dampers with very high slip forces are locked and hence do not dissipate any energy. The results indicate that the overall trend of R_{w2} is similar for all the reference frames irrespective to the number of stories. However, on average, by increasing the number of stories the maximum R_{w2} values are reached at lower slip load ratios. It is evident that the uniform cumulative slip load pattern is usually the most effective pattern in terms of increasing the energy dissipation capacity of the friction-based wall dampers (except for the 3-story frame), while the inverted triangular cumulative pattern is the least efficient. Based on the results in Figure 9, the optimum range of the slip load ratios for 3, 5, 10, 15, and 20-story frames with uniform cumulative slip load distribution is within 0.65-0.95, 0.55-0.85, 0.25-0.45, 0.10-0.30, and 0.05-0.15, respectively.

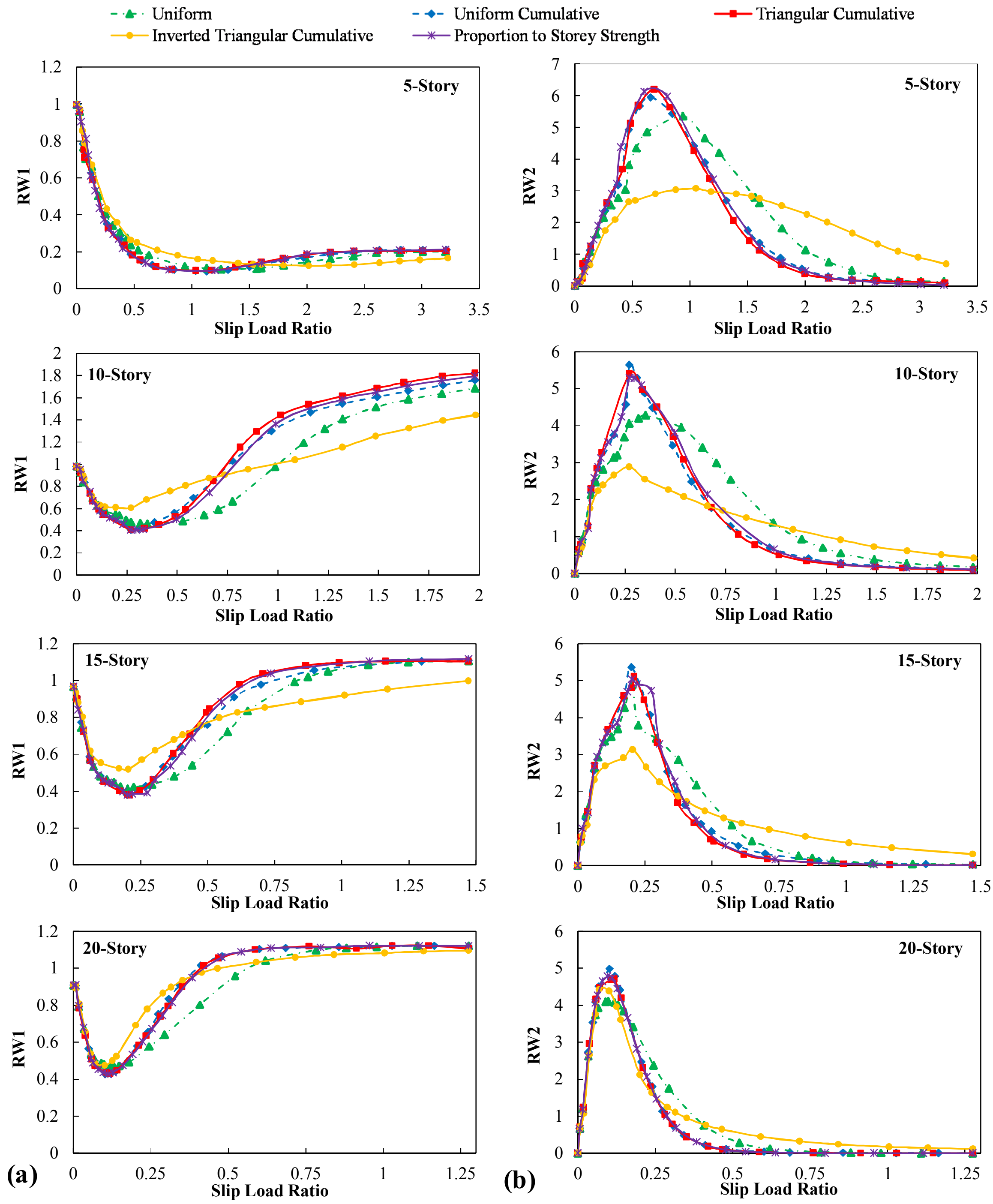

Figure 9. Envelope of energy dissipation parameters (a) $\boldsymbol{R_{w1}}$ and (b) $\boldsymbol{R_{w2}}$ as a function of the slip load ratio, average of the six selected earthquakes

Figure 10 shows the variation of energy dissipation parameter R_{w2} as a function of the slip load ratio for the 10-story and 20-story frames subjected to the six selected real excitation records. It is evident that the amount of energy dissipated in the wall dampers is highly dependent on the input earthquake and the slip load ratio. However, the results show that the range in which the slip load ratio R_{w2} reaches maximum (i.e. the best damper performance) is not significantly affected by the selected design earthquake. This conclusion was confirmed by the results for all the reference frames.

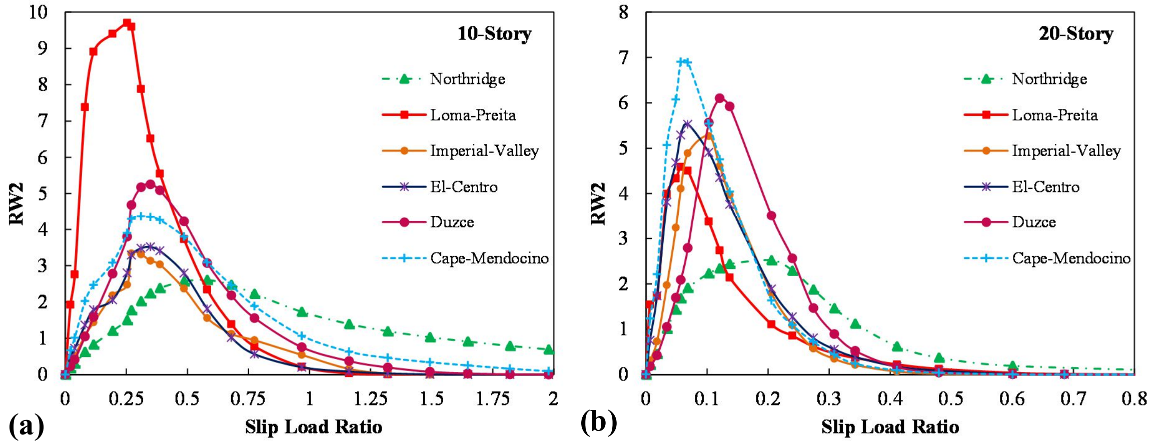

Figure 10. Envelope of $\boldsymbol{R_{w2}}$ energy dissipation parameter for (a) 10-story frame, (b) 20-story frame as a function of the slip load ratio, selected real earthquakes

A PRACTICAL DESIGN METHOD FOR FRICTION WALL DAMPERS

Figure 11 shows the optimum range of the slip load ratios obtained in the previous section as a function of number of stories. The optimum design solutions for low rise buildings tend to a fixed wall system, while for high-rise buildings the best design solutions have lower average slip load ratios. It is shown in Figure 11 that the average value of the optimum slip load ratios can be represented by the following exponential function:

$$R = 1.12e^{-0.11n} \tag{4}$$

where R is the most appropriate slip load ratio and n is the number of stories. The slip load ratio R calculated from Equation 4 is the ratio between the average of the slip loads with uniform cumulative distribution and the average of the story shear strengths. Therefore, the following equation can be used to acquire the more efficient slip load values at each story:

$$F_{si} = \frac{\sum V_{si} \times R}{n(n+1)/2} \times (n+1-i) = \frac{\sum V_{si} \times 1.12e^{-0.11n}}{n(n+1)/2} \times (n+1-i) \tag{5}$$

where n is the number of stories; and F_{si} and V_{si} are the slip load and the story shear. It should be noted that Equation 4 is based on the models considered in this study, and the optimum range might change for the structures with other dynamic characteristics.

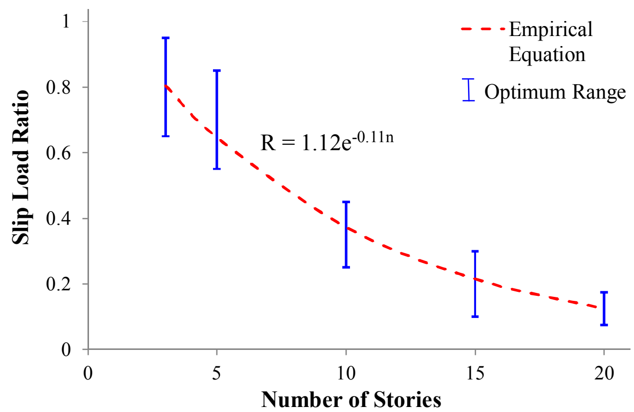

Figure 11. Comparison between the empirical equation and the best analytical slip load range for frames with different number of stories

EFFICIENCY OF THE PROPOSED PRACTICAL DESIGN METHOD

The efficiency of the proposed equation to obtain more efficient design solutions is investigated for 3, 5, 10, 15, and 20-story frames under a set of five design spectrum compatible synthetic earthquakes (see Figure 4). For comparison purposes, the seismic performances of the frames with friction wall dampers designed using Equation 4 are compared with those designed based on the uniform slip load distribution (i.e. conventional design) as well as the frames with fixed panel-to-frame connections. The more efficient slip load values at different stories are calculated by using Equation 5. For a better comparison, the slip load values are scaled in the frames with uniform slip load distribution (without changing the distribution pattern) to have a similar average value in all design solutions.

Figure 12 shows that, in general, the friction-based wall dampers designed with the proposed slip load distribution pattern provide better design solutions with lower maximum drift and roof displacement ratios compared to the conventionally designed wall dampers with uniform slip load distributions. This is especially evident for medium to high-rise buildings. As illustrated in Figure 12, in some cases, using a fixed-wall system can lead to lower inter-story drift and roof displacement demands compared to the frames with friction-based wall dampers. However, fixed-wall systems considerably increase the total base shear and also transfer excessive additional axial loads to the columns and foundation (Figure 12 c and d). To ensure that these added axial force demands are within the load bearing capacity of the columns, the moment-axial load interaction curves of the column sections are investigated. The example in Figure 13 shows that the critical moment-axial load combinations (at the first story) in the 10 and 15-story frames with fixed walls are generally beyond the load bearing capacity of the sections under the set of five synthetic spectrum-compatible earthquakes, while the friction wall dampers designed with the proposed methodology lead to acceptable design solutions. It can also be noted that fixed wall systems under seismic load will produce large tensile forces in the columns that can significantly reduce their moment resistance capacity.

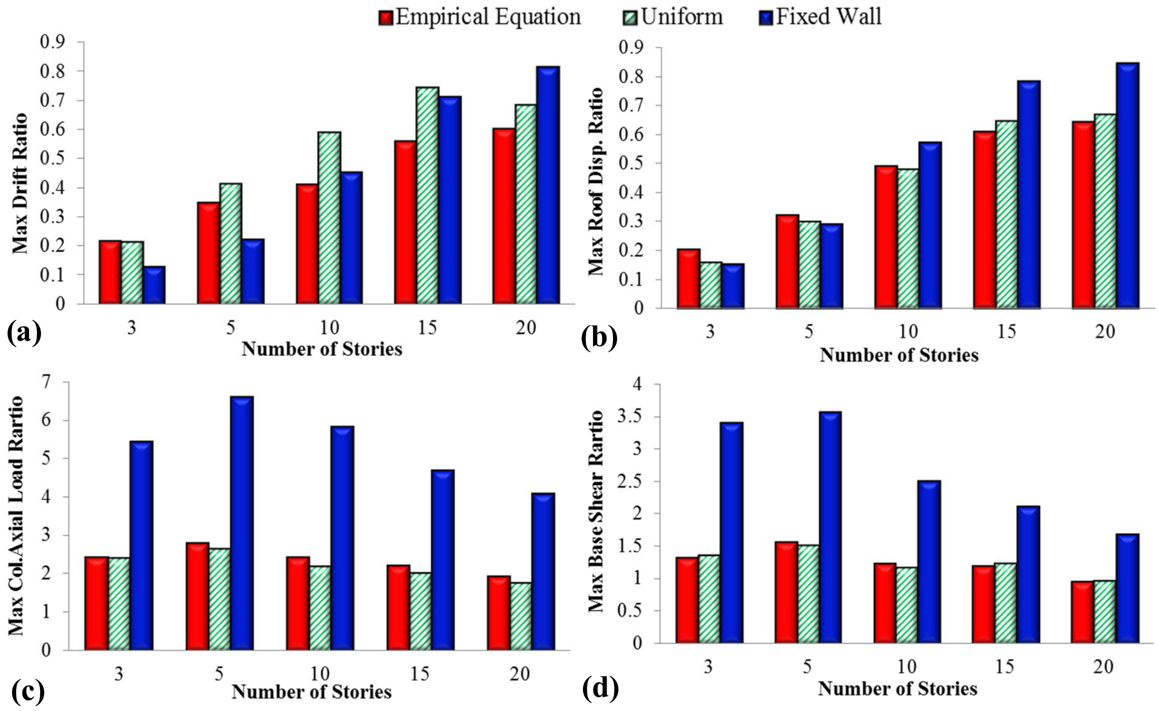

Figure 12. The ratio of (a) maximum drift; (b) maximum roof displacement; (c) maximum column axial load; (d) maximum base shear to the corresponding bare frames, average of five synthetic earthquakes

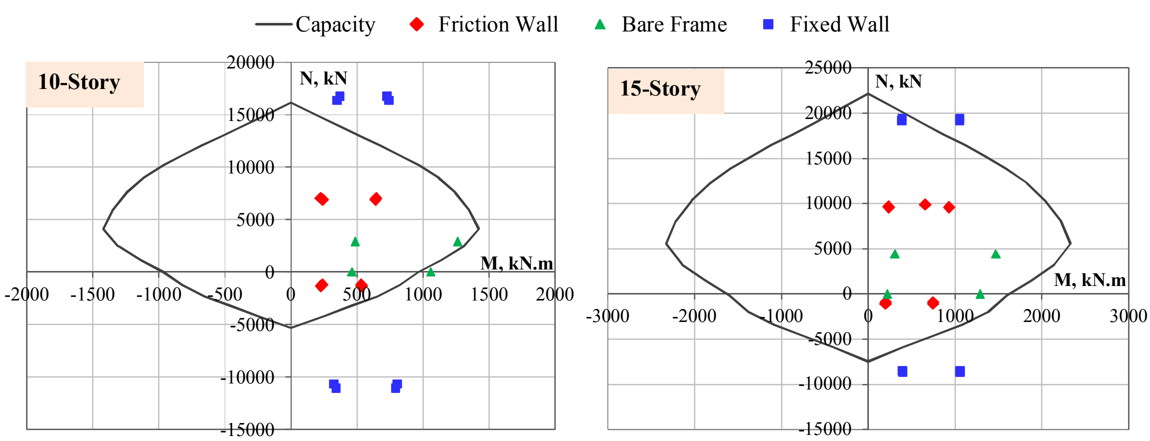

Figure 13. Comparison of the 1st floor column axial load-moment interaction for the bare frames and the frames designed with the empirical equation and fixed wall, average of five synthetic earthquakes

In the case of friction walls designed using the proposed empirical equation the moment-axial load demands on the columns are all within the acceptable range. This is a result of the limits to the story shear introduced by the friction connections. The results also indicate that the performance of the columns of the frames with more efficient design of friction walls can be better than those in the bare frames. The reason is that the increase in axial load of the columns in these frames is accompanied by a decrease in the maximum bending moments due to reduction of inter-story drifts. Figure 14 shows that the proposed slip load distributions in this study can lead to up to 61% higher energy dissipation capacity in the friction devices (i.e. higher R_{w2} factor) and up to 40 % lower energy dissipation demand in the structural elements (i.e. lower R_{w1} factor) compared to the conventional solutions.

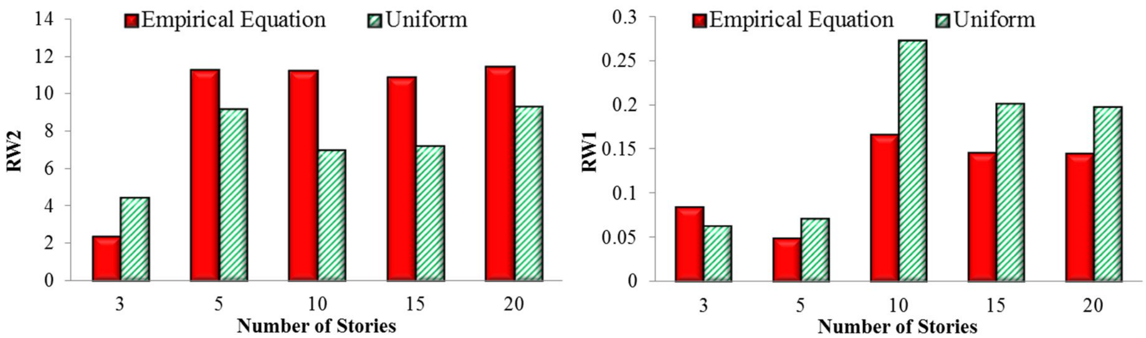

Figure 14. Energy dissipation parameters $\mathbf{R_{w1}}$ and $\mathbf{R_{w2}}$ as a function of number of stories, average of five synthetic earthquakes

GLOBAL DAMAGE INDEX

A linear cumulative damage model is used to calculate the overall damage index of the structure during seismic excitations by taking into account the changes in the energy dissipation capacity of the structure as a function of displacement demands (Miner, 1945; Teran-Gilmore and Jirsa, 2004). In this model it is assumed that the damages caused by plastic excursions are independent, while excursions are identified by using the Rainbow Counting Method suggested by Powell and Allahabadi (1987). In this study the inter-story inelastic deformation is chosen as the basic damage quantity, and the cumulative damage index after N excursions of plastic deformation is calculated using the following equation:

$$DI_i = \sum_{j=1}^{N} \left(\frac{\delta_{pj}}{\delta_y}\right)^C \qquad (6)$$

where (DI_i) is the cumulative damage index at i^{th} story, ranging from 0 for undamaged to 1 for severely damaged stories, N is the total number of plastic excursions, δ_{pj} is the plastic displacement of the j^{th} excursion, δ_y is the ultimate plastic displacement, and c is a structural parameter which accounts for the stability of the hysteretic behavior. In this study, c is considered to be 1.5, as suggested by Cosenza and Manfredi (1996) for damage analysis of reinforced concrete structures.

The global damage index (DI_g) evaluates the damage of the whole structure by considering the weighted average of the story damage indices. The following equation is used to calculate the global damage index of the structures:

$$DI_g = \frac{\sum_{i=1}^{n} DI_i W_{pi}}{\sum_{i=1}^{n} W_{pi}} \tag{7}$$

where n is the number of stories, W_{pi} and DI_i are the dissipated energy and the damage index of the i^{th} story, respectively.

In Figure 15, the global damage indices of the bare frames under the set of five synthetic spectrum compatible earthquakes are compared with the frames with friction-based wall dampers designed using the proposed equation (Equation 5) and the uniform slip load distribution. In general the results indicate that friction-based dampers could significantly improve the seismic performance of the bare frames, especially for low to medium-rise buildings where the global damage index was reduced by up to 91%. Figure 15 (a) shows that friction dampers designed with the proposed equation could reduce the global damage index of the 3, 5, 10, 15 and 20-story frames by 45%, 19%, 43%, 50% and 26%, respectively, compared to conventionally designed dampers.

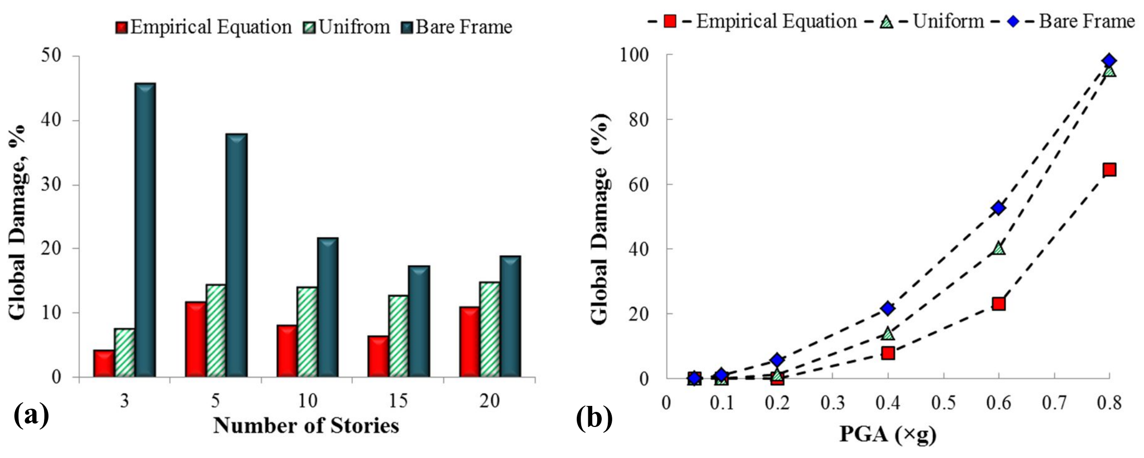

Figure 15. Global damage index of (a) the bare frames compared to the frames with friction-based wall dampers designed using the proposed equation and uniform distribution and (b) the 10-story frame under different earthquake PGA scale factor, average of five synthetic earthquakes

The efficiency of the proposed optimization method is also investigated for different earthquake intensity levels. Figure 15 (b) compares the global damage index (DI_g) of the 10-story bare frame with the frames with friction wall dampers designed using Equation 5 and uniform slip load distributions subjected to the set of five synthetic earthquakes with PGA levels ranging from 0.05 to 0.8 g. It is shown that on average the friction wall dampers with the slip load distribution suggested in this study always exhibit less global damage compared to the frames with conventional friction walls at all PGA levels. The results in Figure 15 (b) imply that the effectiveness of the wall dampers with a uniform slip load distribution was considerably reduced at higher earthquake intensity levels (e.g. PGA> 0.6 g). This is because using equal slip loads at all story levels led to a non-uniform distribution of lateral displacement demands and consequently high local damage concentrated at some of the stories (i.e. soft story failure), while the proposed slip load distribution resulted in a more uniform distribution of story damage.

Although in general the seismic performance of friction wall dampers depends on the frequency content of the input earthquake, number of stories and the earthquake intensity, the outcomes of this study demonstrate that the dampers designed with the proposed method consistently outperform those designed with uniform distribution of slip forces.

SUMMARY AND CONCLUSIONS

In this study, the efficiency of a friction-based wall system was investigated by extensive nonlinear dynamic analyses on 3, 5, 10, 15, and 20-story RC frames subjected to six real and a set of five synthetic design spectrum-compatible earthquakes. To obtain the most efficient height-wise slip load distribution, five different distribution patterns were investigated, including uniform, uniform cumulative, triangular cumulative, inverted triangular cumulative and a distribution proportional to the story shear strengths. Based on the results presented in this paper, the following conclusions can be drawn:

Uniform cumulative slip load distribution is usually the most effective pattern in terms of increasing the energy dissipation capacity of the friction-based wall dampers. However, irrespective to the slip load distributions, there is always an optimum range for the slip load ratios (normalized to the story shear strength) that leads to minimum displacement demands under design compatible earthquakes. For slip load ratios lower than the optimum value, the effectiveness of the dampers can be limited due to the small energy dissipation in the friction devices. Larger slip force ratios, however, may lead to connection lock-ups resulting in a linear elastic response with large dynamic magnification and low energy dissipation. The results show that the optimum range of the slip loads exponentially decreases with the increase of the number of stories.

Based on the results of this study, an empirical equation was proposed to calculate a more efficient slip load distribution for seismic strengthening/design of RC structures with different number of stories. The friction wall systems designed based on the proposed equation was shown to result in lower displacement demands (by up to 30%) and higher energy dissipation capacities (by up to 61%), compared to the conventional systems with a uniform slip load distribution.

It was shown that friction wall dampers designed with the proposed equation can significantly reduce the displacement demands of the bare frames without large increase in base shear. Although friction wall dampers impose additional axial loads to the adjacent columns, it was shown that by using the proposed design method the axial loads generally remain within the capacity of the column sections. However, if fixed panels are added to the bare frame (as a retrofit measure) the maximum axial loads can be well beyond the maximum capacity of the columns.

The results of nonlinear incremental dynamic analyses show that the friction dampers designed with the proposed empirical equation can reduce the global damage index of the RC frames with conventionally designed dampers by up to 43%. While the efficiency of the wall dampers with a uniform slip load distribution was considerably reduced at higher earthquake intensity levels, the suggested design solutions were efficient at all PGA levels.

REFERENCES

Adachi, F., Yoshitomi, S., Tsuji, M. and Takewaki, I., 2013. Nonlinear optimal oil damper design in seismically controlled multi-story building frame, *Soil Dynamics and Earthquake Engineering* **44**, 1–13.

Aiken, I. D., Nims, D. K., Whittaker, A. S. and Kelly, J. M., 1993. Testing of passive energy dissipation systems. *Earthquake Spectra* **9**(3), 335-370.

American Concrete Institute, 2014. *Building code requirements for structural concrete (ACI 318-14) and commentary on building code requirements for structural concrete (ACI 318R-14)*. *American Concrete Institute*, Michigan, USA.

American Society of Civil Engineers (ASCE), 2010. *Minimum Design Loads for Buildings and Other Structures. ASCE/SEI Standard 7-10*, Reston, Virginia.

Cho, C. G. and Kwon, M., 2004. Development and modelling of a frictional wall damper and its applications in reinforced concrete frame structures. *Earthquake Engineering and Structural Dynamics* **33**, 821-838.

Cosenza, E. and Manfredi, G., 1996. Seismic design based on low cycle fatigue criteria. Paper No. 1141, in *Proceedings, 11th World Conference on Earthquake Engineering*, 23-28 June, 1996, Acapulco, Mexico.

Fallah, N. and Honarparast, S., 2013. NSGA-II based multi-objective optimization in design of Pall friction dampers. *Journal of Constructional Steel Research* **89**, 75–85.

Filiatrault, A. and Cherry, S., 1990. Seismic design spectra for friction-damped structures. *Journal of Structural Engineering* **116**(5), 1334-1355.

FitzGerald, T. F., Anagnos, T., Goodson, M., Zsutty, T. , 1989. Slotted bolted connections in aseismic design for concentrically braced connections. *Earthquake Spectra* **5**, 383-391.

Grigorian, C.E., Yang, T.S. and Popov, E. P., 1993. Slotted Bolted Connection Energy Dissipators. *Earthquake Spectra* **9**(3), 491–504.

Hajirasouliha, I. and Doostan, A., 2010. A simplified model for seismic response prediction of concentrically braced frames. *Advances in Engineering Software* **41**(3), 497-505.

Hajirasouliha, I., Asadi, P. and Pilakoutas, K., 2012. An efficient performance-based seismic design method for reinforced concrete frames. *Earthquake Engineering and Structural Dynamics* **41**(4), 663-679.

International Building Code (IBC), 2015. *International Code Council*, Country Club Hills, USA.

Levy, R. and Lavan, O., 2006. Fully stressed design of passive controllers in framed structures for seismic loadings. *Structural and Multidisciplinary Optimization* **32**(6), 485–498.

Miguel, L. F. F., Miguel, L. F. F. and Lopez, R. H., 2016. Simultaneous optimization of force and placement of friction dampers under seismic loading. *Engineering Optimization* **1**, 1-21.

Miner, M. A., 1945. Cumulative damage in fatigue. *Journal of Application Mechanics* **12** (3), 59–164.

Moreschi, L .M. and Singh, M. P., 2003. Design of yielding metallic and friction dampers for optimal seismic performance. *Earthquake Engineering and Structural Dynamics* **32**, 1291-1311.

Nikoukalam, M. T., Mirghaderi, S. R. and Dolatshahi, K. M., 2015. Analytical study of moment-resisting frames retrofitted with shear slotted bolted connection. *Journal of Structural Engineering, ASCE* **141**(11), 4015-4019.

Pall, A. S. and Marsh, C., 1982. Response of friction damped braced frames. *ASCE, Journal of Structural Division* **108**, 1313-1323.

Pall, A. S. and Pall, R. T., 2004. Performance-based design using pall friction dampers; an economical design solution. Paper No. 1955, in *Proceedings, 13th World Conference on Earthquake Engineering*, 1-6 August, 2004, Vancouver, Canada.

Park, J. H., Kim, J. and Min, K.W., 2004. Optimal design of added viscoelastic dampers and supporting braces. *Earthquake Engineering and Structural Dynamics* **33**(4), 465-484.

Patro, S. K. and Sinha, R., 2010. Seismic performance of dry-friction devices in shear-frame buildings. *Journal of Civil Engineering and Architecture* **4**(12).

Petkovski, M. and Waldron, P., 2003. Optimum friction forces for passive control of the seismic response of multi-story Buildings. in *Proceedings, 40 years of European Earthquake Engineering SE40EEE*. 30 August-03 September, 2003, Ohrid, Macedonia.

Powell, G. H., and Allahabadi, R., 1987, Seismic damage prediction by deterministic methods: concepts and procedures, *Earthquake Engineering and Structural Dynamics* **16**, 719-734.

Prakash, V., Powell, G. H. and Campbell, S., 1993. *DRAIN-2DX base program description and user guide*, Version 1.10. University of California, Berkeley, California.

Sasani, M. and Popov, E. P., 1997. *Experimental and analytical studies on the seismic behaviour of lightweight concrete panels with friction energy dissipaters*, *Earthquake Engineering Research Centre*, Report No. UBC/EERC-97/17, Berkeley, California.

Sasani, M. and Popov, E. P., 2001. Seismic energy dissipaters for RC panels; analytical studies. *Journal of Engineering Mechanics* **127**(8), 835-843.

Sonmez, M., E. Aydin, and T. Karabork. 2013. Using an artificial bee colony algorithm for the optimal placement of viscous dampers in planar building frames. *Structural and Multidisciplinary Optimization* **48**, 395–409.

Soong, T. T., and Costantinou, M. C., 2014. *Passive and active structural vibration control in civil engineering, Springer* **345**.

Symans, M. D., Charney, F., Whittaker, A., Constantinou, M., Kircher, C., Johnson, M. and Mcnamara, R. 2008. Energy dissipation systems for seismic applications: current practice and recent developments. *Journal of Structural Engineering* **134**(1), 3–21.

Takewaki, I., 2011. Building control with passive dampers: *optimal performance-based design for earthquakes*. John Wiley and Sons (Asia) Books, Singapore, 51-75.

Teran-Gilmore, A. and Jirsa, J. O., 2004. The concept of cumulative ductility strength spectra and its use within performance-based seismic design. *ISET Journal of Earthquake Technology* **41**(1), 183-200.

Vanmarke, E. H., 1976. *SIMQKE: A program for artificial motion generation, user's manual and documentation*. Department of Civil Engineering, Massachusetts Institute of Technology.

Whittle, J.K., Williams, M.S., Karavasilis, T.L. and Blakeborough, A., 2012. A comparison of viscous damper placement methods for improving seismic building design, *Journal of Earthquake Engineering* **16**, 540-560.

Wu, B., Zhang, J., Williams, M. S., Ou, J., 2005. Hysteretic behaviour of improved pall-typed frictional dampers. *Engineering Structures* **27**, 1258-1267.